# Effect of Torrefaction on Bio-oil Upgrading over HZSM-5. Part 1: Product Yield, Product Quality, and Catalyst Effectiveness for Benzene, Toluene, Ethylbenzene, and Xylene Productio...

**ARTICLE** *in* ENERGY & FUELS · JANUARY 2013

Impact Factor: 2.79 · DOI: 10.1021/ef301694x

energy&fuels

Article

pubs.acs.org/EF

# Effect of Torrefaction on Bio-oil Upgrading over HZSM-5. Part 1: Product Yield, Product Quality, and Catalyst Effectiveness for Benzene, Toluene, Ethylbenzene, and Xylene Production

Roger N. Hilten,* Richard A. Speir, James R. Kastner, Sudhagar Mani, and K. C. Das

College of Engineering, Driftmier Engineering Center, University of Georgia, Athens, Georgia 30202, United States

**ABSTRACT:** A three-step bio-oil production process involving torrefaction pretreatment (at 225, 250, or 275 °C with a 20 min hold time), pyrolysis (at 500 °C with two heating rates), and secondary catalytic processing over HZSM-5 (at 400, 450, or 500 °C) was studied to determine process effects, particularly of torrefaction, on the yield of liquid and aromatic hydrocarbons and the quality of upgraded bio-oil. When bio-oils derived from torrefied biomass were catalytically cracked, average yields (%, w/w of feed) of reactor char (100% reduction), catalyst coke (21.4%), and catalyst tar (8.1%) were significantly reduced relative to the best-case conditions using non-torrefied feedstock. The reduction in coke (%, w/w of feed) as a result of torrefaction was 28.5% relative to the respective control for slow-pyrolysis bio-oil upgrading and 34.9% for fast-pyrolysis bio-oil upgrading. The concentration of aromatic product (benzene, toluene, ethylbenzene, and xylene, i.e., BTEX) was highest at 95 g $L^{-1}$ for upgraded (at 500 °C) fast-pyrolysis bio-oil derived from biomass torrefied at 275 °C. Catalyst effectiveness for BTEX production significantly increased with increased torrefaction and catalytic cracking temperatures.

## INTRODUCTION

Catalytic cracking has been shown to improve the quality of pyrolysis oils generated from a variety of high oxygen content feedstocks, including rice husks, rice straw,[1] pine wood,[1−3] maple wood,[4,5] and poplar wood.[6] The cracking process was developed by the petroleum industry to crack and rearrange high boiling, high-molecular-weight petroleum crude oil fractions to predominantly gasoline and other light hydrocarbons.[7] Cracking catalysts generally used for treating biomass-derived oils have been acidic zeolites with ion-exchange capacity and size-selectivity functionality that have been shown to effectively deoxygenate bio-oil feedstocks and form desirable end-products, including small alkanes and aromatics.[4,7,8] However, catalyst coking is extensive, and many studies have sought methods to reduce coke formation.[3,7,9] Adjaye and Bakhshi[4,5] attempted to catalytically crack fast-pyrolysis bio-oil with five different catalysts (ZSM-5, H-Y-zeolite, H-mordenite, silicalite, and silica-alumina). The yield of organic liquid product was highest with ZSM-5 (34%, w/w of feed), although the coke yield was as high as 29% (w/w of feed). Vitolo et al.[10] indicated much more modest levels of coke (4.2−6.7%, w/w of feed) using HZSM-5 to process Swedish pine at 500 °C. According to Rao et al.,[11] the amount of coke generated during modern crude oil processing is around 5% (w/w of crude oil feed). As long as the amount of coke generated from bio-oil processing can remain in the range for crude oil processing, the transition to processing biomass-derived feedstock in existing petroleum units will not be problematic.

One way to minimize coke formation on zeolite catalysts is to remove coke precursors from the oil prior to upgrading. Compounds that are thought to promote coke formation include aldehydes, oxyphenols, furfurals, and lignin-derived oligomers.[6,12] Other studies involving hydrotreating of bio-oil[13−16] have indicated that the carbohydrate fraction is a major contributor to coke formation. There are currently few studies that attempt to remove coke precursors from bio-oil prior to upgrading. Gayubo et al.[17] removed the pyrolytic lignin fraction of bio-oil prior to passing vapors across a catalytic bed and observed improvement in catalyst longevity at the cost of reduction in yield. Pretreatment of biomass by torrefaction prior to pyrolysis is another potential way to remove coke precursors from bio-oil prior to upgrading and, thus, reduce coke formation and improve bio-oil quality.

Biomass torrefaction is a low-temperature pyrolysis process, similar to coffee roasting, in which the biomass is heated in an inert environment ($N_2$) from 200 to 320 °C. Torrefaction generates a hydrophobic, friable solid biomass that requires less energy for grinding relative to untorrefied biomass.[18] Improved grinding is of particular benefit for fluidized-bed pyrolysis or gasification, where small particle sizes are required for proper fluidization. Torrefied biomass has lower elemental oxygen content (CO, $H_2O$, and $CO_2$ are emitted during torrefaction) compared to untreated biomass[19], meaning that less oxygen is available for incorporation into products.

Additionally, torrefaction drives off other reactive and acidic intermediate components, including acids (e.g., acetic, formic, and propionic) and aldehydes (e.g., formaldehyde, hydroxyacetaldehyde, acetaldehyde, and furfural).[18,20−22] Meng et al.[23] observed the effect of torrefaction pretreatment on the chemistry of fast-pyrolysis bio-oil, noting that torrefaction resulted in a bio-oil with a larger fraction of pyrolytic lignin with the implication that torrefaction effectively removed hemicellulose and some cellulose components. Although some reactive gases produced during the torrefaction phase of pyrolysis have been shown to generate coke on acid catalysts,

**Received:** October 17, 2012
**Revised:** January 4, 2013
**Published:** January 4, 2013

   dx.doi.org/10.1021/ef301694x | *Energy Fuels* 2013, 27, 830−843

Table 1. Feedstock Characteristics for Torrefied and Untorrefied PC Biomass

| | feedstock characteristics (%, w/w, db) | | | | |
|---|---|---|---|---|---|
| parameter | PC (average ± 95% CI) | PC T100 (average ± 95% CI) | PC T225 (average ± 95% CI) | PC T250 (average ± 95% CI) | PC T275 (average ± 95% CI) |
| yield[a] | 100 ± N/A | 86.0 ± N/A | 71.2 ± N/A | 69.7 ± N/A | 55.6 ± N/A |
| dry basis | | 100 ± N/A | 82.8 ± N/A | 81.1 ± N/A | 64.7 ± N/A |
| moisture[b] | 14.0 ± 0.32 | 0.03 ± 0.02 | 0.48 ± 0.28 | 0.35 ± 0.10 | 0.01 ± 0.02 |
| volatile matter | 82.0 ± 0.42 | 81.4 ± 0.02 | 80.0 ± 0.22 | 77.9 ± 1.20 | 72.3 ± 0.47 |
| ash | 0.2 ± 0.03 | 0.30 ± 0.04 | 0.36 ± 0.03 | 0.39 ± 0.05 | 0.20 ± 0.16 |
| fixed carbon | 17.9 ± 0.39 | 18.3 ± 0.02 | 19.6 ± 0.24 | 21.7 ± 1.15 | 27.5 ± 0.31 |
| C | 46.9 ± 0.2 | 46.9 ± 0.2 | 48.3 ± 0.5 | 48.4 ± 0.1 | 53.3 ± 0.6 |
| H | 5.98 ± 0.1 | 5.98 ± 0.1 | 5.88 ± 0.1 | 5.83 ± 0.1 | 5.6 ± 0 |
| N | 0.45 ± 0.1 | 0.45 ± 0.1 | 0.88 ± 0.2 | 0.82 ± 0.1 | 1 ± 0.3 |
| S | 0 ± 0 | 0 ± 0 | 0 ± 0 | 0 ± 0 | 0 ± 0 |
| O[c] | 46.3 ± 0.2 | 46.3 ± 0.2 | 44.6 ± 0.2 | 44.6 ± 0.1 | 39.9 ± 0.5 |
| HHV[d] (MJ kg$^{-1}$) | 18.6 ± 0.1 | 18.6 ± 0.1 | 19.1 ± 0.1 | 19.1 ± 0.1 | 21.1 ± 0.3 |

[a]Yields are calculated versus air-dried PC biomass. [b]Wet basis. [c]By difference. [d]Calculated following the study by Channiwala and Parikh.[33]

leading to deactivation,[12,24] and despite the fact that the 2008 NSF/DOE Roadmap[25] has indicated that the impact of torrefaction on thermochemical processing should be investigated, to date, no research has been performed to determine the effect of torrefaction as a pretreatment for pyrolysis followed by catalytic cracking of produced bio-oil. Torrefaction, when coupled with pyrolysis and catalytic cracking, could provide synergistic effects not realized with pyrolysis and catalytic treatment alone. In particular, the removal of volatile materials during torrefaction could have a positive effect on subsequent catalytic processing and product quality.

Hemicellulose decomposition has been proposed to occur in the temperature range from 200 to 300 °C, with drying occurring prior to 200 °C. For cellulose, the range of decomposition is 300−400 °C, and for lignin, the range of decomposition is 250−500 °C.[26] Thus, in the normal temperature range for torrefaction (200−320 °C), biomass is effectively dried and hemicellulose is devolatilized and decomposed along with some cellulose and lignin.[27] During torrefaction, a variety of compounds are evolved, including acetic acid, which is derived from the deacetylation of the xylan component of hemicellulose.[23,24] Several hemicellulose-derived compounds that decompose to coke in the subsequent upgrading step, including acetyl groups that form acetic acid and other short-chain carboxylic acids, are removed via torrefaction.[21,28,29] Joo et al.[30] showed that formaldehyde, another hemicellulose-derived compound, effectively deactivated strong acid sites on HZSM-5 catalysts. Part 2 of the current study (10.1021/ef301695c) further investigated the changes in catalyst properties and function as a result of processing bio-oil with varying levels of coke precursors. Pommer et al.[21] observed measurable concentrations of aldehydes, including formaldehyde, acetaldehyde, syringaldehyde, hydroxyacetaldehyde, and furfural, during torrefaction. In addition, after upgrading bio-oil from non-torrefied feedstock, residual acetic acid ends up in the product, causing high acidity (low pH). Thus, it is proposed that a hemicellulose-depleted feedstock will result in pyrolysis oils containing less acetic acid and other reactive compounds and result in less coke formation during subsequent catalytic upgrading. The main objective of this study was to investigate the catalytic upgrading of fast- and slow-pyrolysis bio-oil generated from torrefied pine wood to determine the effects of torrefaction on the yield and quality of products and byproducts.

## EXPERIMENTAL SECTION

A multi-step process was used to generate high-quality bio-oil from loblolly pine. Steps included feedstock pretreatment (via torrefaction), pyrolysis (fast and slow heating rates), and secondary catalytic cracking. Torrefaction was performed in a pilot-scale (500 kg per batch) rotating kiln torrefaction unit. Torrefied feedstock was pyrolyzed under fast-pyrolysis conditions (<5 s reaction time) in a continuous flow fluidized-bed pyrolysis unit (FBPU). Slow pyrolysis was performed in a batch slow-pyrolysis unit (BSPU). For catalytic cracking, a fixed-bed plug-flow reactor (PFR) unit was used to process bio-oil generated via the fast pyrolysis of pine chip (PC) or torrefied pine chip (TPC) biomass.

Loblolly pine biomass was supplied by Plum Creek Timber Company (Athens, GA) in the form of delimbed and debarked logs harvested in northeastern Georgia. Logs were then cut into sections prior to being chipped in a Vermeer 1230 brush chipper (Vermeer Corporation, Pella, IA). Material was then sorted in a Royer model 42 power screener (Royer Industries, Oshkosh, WI) using a 0.64 cm screen to collect rejected material. Particles larger than 5 cm were hand-removed. Chipped biomass was left to air-dry in a covered, open shed for 6 months prior to further processing.

**Biomass Pretreatment.** Biomass pretreatment via torrefaction was performed at 225, 250, and 275 °C, a commonly used temperature range for the partial or complete removal of hemicellulose, in a pilot-scale rotary kiln. During the torrefaction process, approximately 100 kg of air-dried pine chips (2−5 cm particle size) were loaded into the rotary kiln. The kiln was a 3 m$^3$ octagonal-shaped mild steel reactor externally heated by a 22.9 MW (1.3 MMBTU h$^{-1}$) natural gas burner. The volume of the pine chips comprised less than 1 m$^3$ of the reactor volume. The axially rotating system had ports allowing for inert gas input through one end and exhaust output from a 41 cm pipe at the opposite end. Nitrogen was supplied concentric to the axis of rotation via a rotary union inlet from a liquid tank at 8−17 m$^3$ h$^{-1}$. An external motor controlled by a TECO Speecon 7300 CU controller (TECO Electric and Machinery Co., Taiwan) was used to maintain a rotation speed at 0.75 rpm, selected to minimize size reduction of the material and fine dust formation. The system temperature was regulated by a Honeywell UDC2500 controller (Fort Washington, PA), allowing for a set point temperature to be adjusted with a proportional−integral−derivative (PID) function relayed to the Maxon model 400 natural gas burner (Honeywell, Muncie, IN). The burner was equipped with a Honeywell burner control ultraviolet (UV) flame amplifier. The temperature used for maintaining the set point was monitored at the wall of the reactor. Additional temperature readings were recorded at 15, 30, and 45 cm from the axis of rotation inside the reactor to analyze the temperature distribution in the feedstock. An additional controller monitored the kiln upper set point with a thermocouple at the opposite end. Generated vapors were incinerated with a Midco

Incinomite 29−235 kW (0.1−0.8 MMBTU $h^{-1}$) burner (Midco International, Chicago, IL) before exhausting. Once each end temperature was reached, a holding time of 20 min was maintained to drive complete devolatilization of components. After torrefaction, the resulting torrefied feedstocks (PC T225, PC T250, and PC T275) were characterized (see Table 1), ground to 1−2 mm, then subjected to fast pyrolysis at 500 °C, or left in chip form for slow-pyrolysis processing, as described in the following section.

**Bio-oil Production.** Bio-oil was generated by pyrolyzing oven-dried (105 °C for 4 h) or torrefied (225, 250, or 275 °C) PC biomass at 500 °C in the FBPU (minimum heating rate of >100 °C $s^{-1}$) or the BSPU (0.13 °C $s^{-1}$ heating rate). Prior to fast pyrolysis, the biomass particle size was reduced in a hammer mill to 1−2 mm. The FBPU consisted of a volumetric auger feeder, a fluidized-bed riser reactor (61 cm length by 4.75 cm inner diameter), two sequential cyclonic solid separators, a hot gas filter (5 $\mu$m pore size), and a water-cooled shell and tube condensing system maintained at 20 °C. Biomass feed was supplied at ∼500 g $h^{-1}$ to the reactor (maintained at 500 °C), where the feed contacted hot fluidized quartz sand (0.255 mm mean diameter) in 20 L $min^{-1}$ preheated $N_2$. The volumetric biomass feeder was weighed prior to and after runs to determine the total amount of biomass fed for yield calculations. The batch slow-pyrolysis reactor used was a cubical stainless-steel (316L) container with dimensions of 20 cm height × 20 cm width × 20 cm diameter. Two 1.3 cm ports allowed for the introduction of inert gas and the removal of evolved gases and vapors. For slow-pyrolysis runs, approximately 3 kg of dry pine chips was placed in the reactor and the reactor was placed in a single set point electric furnace (Thermolyne model 30400, BarnStead International, Dubuque, IA). A low heating rate (8 °C $min^{-1}$) was applied until the reactor reached a final internal temperature of 500 °C, and evolved vapors were condensed in an ice bath vapor trap. The two-phase liquid obtained was separated in a gravity separation funnel. The heavier, non-aqueous lower phase was considered the product. Subsamples of condensed bio-oil from fast and slow pyrolysis (heavier organic phase) were taken for analysis, while the remaining sample was used in the subsequent catalytic cracking process described below.

**Bio-oil Catalytic Cracking.** Previously produced and phase-separated (slow pyrolysis only) bio-oil was injected continuously into the PFR maintained at 400, 450, or 500 °C in a tube furnace. The PFR consisted of a 2.4 cm inner diameter reactor with a 38 cm length. A 15 cm preheater section, maintained at the reaction temperature, was incorporated into the reactor to ensure that bio-oil was in vapor phase prior to crossing a 10 g catalyst bed (28.5 $cm^3$) that was held in place by stainless-steel screens and quartz wool above and below the bed. Bio-oil was pumped using a peristaltic pump that maintained a feed rate of 1.5 $cm^3$ $min^{-1}$ (∼100 g $h^{-1}$ at an average bio-oil feedstock density of 1.1 g $cm^{-3}$) corresponding to a weight hourly space velocity (WHSV, $h^{-1}$) of 10 $h^{-1}$. WHSV was calculated as the mass flow rate (g $h^{-1}$) of liquid feed divided by the catalyst mass (g). These reaction conditions corresponded to a liquid hourly space velocity [LHSV = reactant liquid flow rate ($cm^3$ $h^{-1}$)/reactor volume ($cm^3$)] of 3.2 $h^{-1}$. The catalyst/oil ratio (C/O, weight of catalyst divided by the weight of oil fed) ranged from 0.34 to 0.65. The catalyst contact time (i.e., duration of experiments) was calculated as 3600/(WHSV × C/O) and ranged from 554 to 1058 s. Given a carrier gas flow rate of 50 $cm^3$ $min^{-1}$, the gas phase residence time in the catalytic zone ($V$ = 28.5 $cm^3$) was approximately 34 s. Under these conditions, no reactor plugging was observed.

**Catalyst Preparation.** The catalyst, HZSM-5, was produced by calcining $NH_4$-ZSM-5 (Zeolyst International, CBV 5524 G) at 550 °C for 4 h in air to produce the hydrogen form, HZSM-5, resulting in stronger acid pore sites. The pH was measured by mixing catalyst in water at a 50:50 ratio and then measuring the pH of the water using a standard pH probe. As a result of the calcining process, the pH was reduced from 4.98 to 3.06. The $NH_4$-ZSM-5 catalyst was received from the manufacturer as a fine powder. To minimize the pressure drop across the catalyst bed, the catalyst was granulated by mixing with water, drying, crumbling, and sieving to the desired size, ∼2−4 mm.

After calcination, granulation, and drying, catalyst surface characteristics (surface area, average pore radius, and pore volume) were determined using a surface area analyzer (Quantachrome Autosorb, model 1-C, Boynton Beach, FL) by measuring $N_2$ adsorption/desorption isotherms. The adsorption and desorption isotherms were obtained at −196 °C (77 K) with the Brunauer−Emmett−Teller (BET) surface area calculated from the linear portion of the multipoint BET plot. The micropore volume and external surface area were evaluated using the *t*-plot method, and the pore size distribution was obtained using the Brunauer−Joyner−Halenda (BJH) model. Characteristics of as-received and prepared catalyst are provided in Table 2.

**Table 2. Characteristics of As-Received and Prepared HZSM-5 Catalyst**

| property | as received | prepared |
|---|---|---|
| cation form | $NH_4^+$ | $H^+$ |
| Si/Al | 50 | 50 |
| particle size (mm) | 0.005 | 2−4 |
| surface area ($m^2$ $g^{-1}$) | 425 | 345 |
| average pore radius (Å) | N/A | 10.8 |
| pore volume ($cm^3$ $g^{-1}$) | N/A | 0.19 |

Including control samples that were dried at 100 °C and subsequently subjected to the catalytic process, 32 bio-oil types were produced and labeled by pretreatment (torrefaction) temperature (T100, T225, T250, or T275), pyrolysis heating rate [fast-pyrolysis oil (FPO) or slow-pyrolysis oil (SPO)], and catalytic upgrading temperature (U400, U450, or U500). Each process condition was run in triplicate for a total of 96 samples. Intermediate bio-oils produced from pyrolysis, FPO and SPO, and torrefaction follow by pyrolysis (SPO and FPO T225, T250, and T275) were also analyzed to determine the effect of torrefaction on intermediate bio-oil characteristics.

The product yield (%, w/w) for each step, including torrefaction, pyrolysis, and catalytic cracking, was determined as the weight change of the collection vessel divided by feedstock input. For both fast and slow pyrolysis, the amount of liquid collected did not necessarily represent the total amount of condensable vapor, particularly for fast-pyrolysis runs, but only the amount condensed at specific process conditions. For fast-pyrolysis runs, the shell and tube condenser was set at 21 °C such that a fraction of low boiling components was not collected. However, when all components were collected, the yield of liquid product was ∼60%. The phase yield, oily and aqueous, was determined by weighing gravity-separated fractions.

The combined yield of catalytic cracking byproducts, including tar, catalyst coke, and reactor char, was quantified by measuring the change in the weight of the catalytic cracking reactor. Yields of individual byproduct components, coke, tar, and char (by difference), were also determined. Tar was considered to be the toluene/acetone/methanol-soluble material adhered to the catalyst and was quantified by washing the catalyst with a solvent mixture containing equal parts toluene, acetone, and methanol (TAM) after catalytic runs, drying the catalyst, and measuring the change in mass. Catalyst coke formation was determined by heating the washed catalyst in a thermogravimetric analyzer (TGA) at 10 °C $min^{-1}$ to 650 °C under oxygen flow. The change in the mass of catalyst was assumed to be due to the complete combustion of coke. The weight of reactor char was then determined as the difference between the reactor weight change and combined coke and tar weight. All yields were calculated relative to dry PC feedstock, unless otherwise noted.

**Product Characterization.** Solid materials, including biomass, torrefied biomass, and pyrolysis char, were subsampled and analyzed. Other solids generated during catalytic cracking, including reactor char, catalyst coke, and tar, were not analyzed compositionally, only quantified. The yield of noncondensable gas was determined by difference.

Feedstock and products were analyzed by an assortment of methods. Biomass feedstock was analyzed for proximate composition (moisture, volatile matter, ash, and fixed carbon), and elemental

Table 3. Yield of Material after Pretreatment and Pyrolysis

| | yield (%, w/w, pretreated biomass) | | | | | | | |
|---|---|---|---|---|---|---|---|---|
| | fast pyrolysis | | | | slow pyrolysis | | | |
| fraction | T100 | T225 | T250 | T275 | T100 | T225 | T250 | T275 |
| oil | 22.4 | 13.8 | 13.8 | 11.0 | 8.5 | 8.1 | 7.4 | 7.8 |
| aqueous | 0.0 | 0.0 | 0.0 | 0.0 | 34.1 | 35.1 | 34.3 | 27.0 |
| char | 21.0 | 17.8 | 31.1 | 66.5 | 29.6 | 29.4 | 30.2 | 37.8 |
| gas | 56.6 | 68.4 | 55.1 | 22.4 | 27.3 | 26.7 | 26.1 | 26.1 |

composition (CHNS-O). The initial quality of bio-oils was assessed by measuring CHNS-O and calculating molar $H/C_{eff}$ and O/C ratios, which indicate fuel applicability and the level of deoxygenation, respectively, as a result of secondary catalytic processing. $H/C_{eff}$ was calculated as follows:

$$H/C_{eff} = \frac{\text{mol of H} - 2 \times \text{mol of O}}{\text{mol of C}} \quad (1)$$

Storage stability was assessed in a differential scanning calorimeter (DSC), in which the oxidation onset temperature (OOT) was determined following Hilten et al.[32] and ASTM E2009, "Standard Test Method for Oxidation Onset Temperature of Hydrocarbons by Differential Scanning Calorimetry". Using the method, oils were heated from room temperature to 250 °C under an oxygen environment. At a material-specific temperature, combustion (oxidation) began. Oxidation onset was determined by extrapolating the baseline and slope of the oxidation peak. The point of intersection was considered the oxidation onset temperature. A higher temperature at the onset of oxidation implies greater storage stability (i.e., greater resistance to oxidation during accelerated aging).

Chemical composition was determined using calibrated gas chromatography–mass spectrometry (GC–MS) and high-performance liquid chromatography (HPLC) methods. The calibrated GC–MS method was used to determine the concentration of proposed products, including benzene, toluene, ethylbenzene, and xylene (collectively, BTEX) products, based on six-point calibrations with pure compound mixtures with an internal standard, heptane. Upon calculating peak areas relative to heptane and using the calibration factors from the standard calibration curve, the concentration of BTEX in the product liquid was found for all samples from each process condition combination. Product yields of benzene, toluene, ethylbenzene, *p*-, *m*-, and *o*-xylene, total BTEX, and other non-BTEX compounds were found relative to the amount in the feed bio-oil. The HPLC system (Shimadzu) was used to determine the concentrations ($g\ L^{-1}$) of major water-soluble acids, including acetic and formic acids, using a calibrated method. Aqueous samples for HPLC analysis were generated by thoroughly mixing oily phase bio-oil with water at a 1:1 ratio, centrifuging the mixture, and then taking a subsample of the upper aqueous phase for analysis.

**Catalyst Effectiveness.** Catalyst effectiveness was determined as in the study by Adjaye and Bakhshi.[5] The study defined $C_{eff}$ as follows:

$$C_{eff} = Y_i S_i \quad (2)$$

In eq 2, $Y_i$ is the yield of product $i$ and is defined as

$$Y_i\ (\text{wt \%}) = \text{product (g)/bio-oil fed (g)} \times 100 \quad (3)$$

In eq 2, $S_i$ is the selectivity and is calculated by

$$S_i = \text{desired product (wt \%)/undesired product (wt \%)} = \text{product (wt \%)/(bio-oil fed (wt \%) − product (wt \%))} \quad (4)$$

Selectivity was found using eq 4 for product liquid, individual BTEX compounds (benzene, toluene, ethylbenzene, *p*-xylene, and *m*-xylene), and combined BTEX.

Calculated using eq 2, $C_{eff}$ is a percent. For this study, yields and selectivities of liquid and BTEX products were used to calculate catalyst effectiveness, $C_{eff,liquid}$ and $C_{eff,BTEX}$, respectively. $C_{eff}$ was calculated as means to determine which pretreatment and reaction conditions were optimal in the production of liquid and BTEX products.

**Statistical Design.** The experiment was designed such that three-way analysis of variation (ANOVA) could be used to determine the effects of three factors, including pretreatment temperature (four levels at 100, 225, 250, and 275 °C, denoted as T100, T225, T250, and T275), pyrolysis heating rate (two levels at 0.13 or 100 °C $s^{-1}$, denoted as SP or FP for slow pyrolysis and fast pyrolysis), and catalytic cracking temperature (four levels at 400, 450, and 500 °C and the control denoted as U400, U450, U500, and CTRL), on yields and product composition and quality. The null hypothesis for all analyses was that factors at any level had no effect on product yield, product composition, or catalyst characteristics. Rejection of the null hypothesis was concluded at $p$ values less than a level of significance, $\alpha = 0.05$. The Holm–Sidak or Tukey method of multiple comparisons was used to compare the effects of levels for each factor.

## RESULTS AND DISCUSSION

**Effect of Torrefaction on Solid Feedstock.** Yields of solid material at T100, T225, T250, and T275 were 86.0, 71.2, 69.7, and 55.7% (w/w of air-dried PC biomass), respectively, after a hold time of 20 min, as shown in Table 1. As expected, the solid product (torrefied biomass) yield significantly ($p < 0.001$) decreased with an increasing torrefaction temperature as a result of greater volatilization. As indicated in Table 1, the volatile matter remaining was indeed lower for PC having undergone higher temperature torrefaction. At the same time, fixed carbon and elemental carbon in the solid increased from 17.9 to 27.5% (w/w) and from 46.9 to 53.3% (w/w), respectively, for PC versus PC T275, an indication of partial carbonization. Concurrently, the oxygen content was reduced from 46.3 to 39.9% (w/w).

**Effect of Torrefaction on Pyrolysis Yield.** With less volatile matter remaining, the liquid yield from pyrolysis of torrefied material showed a significant linear decrease with an increasing pretreatment temperature ($p < 0.001$) from 22.4% at T100 to 11.0% at T275 for FP processing and from 8.5 to 7.8% for SP processing. The char yield, on the other hand, increased significantly ($p < 0.001$) from 21.0% at T100 to 66.5% at T275 for FP and from 29.6 to 37.8% for SP. Table 3 provides additional yield results for the pyrolysis processes relative to pretreatment conditions. Aqueous phase and oily phase liquid showed a significant inverse relationship with the pretreatment temperature (i.e., the liquid yield was reduced with an increasing temperature). Concurrently, the noncondensable gas yield increased significantly with an increasing pretreatment temperature. Figure 1 provides liquid yield versus dry PC. For both fast and slow pyrolysis, there was a linear decrease in the yield for oily phase liquid with an increasing pretreatment temperature.

**Effect of Torrefaction on Catalytic Cracking Yield.** Torrefaction had a significant effect on the yield of all products of catalytic cracking, including liquid product (oily and


dx.doi.org/10.1021/ef301694x | Energy Fuels 2013, 27, 830–843

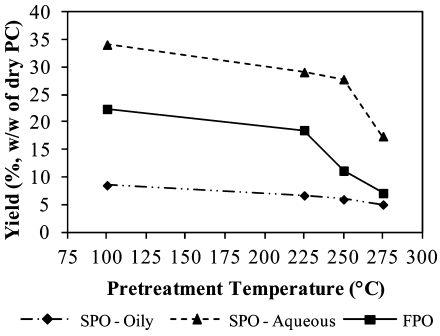


**Figure 1.** Yield of oily and aqueous phase oil from pyrolysis of torrefied PC biomass relative to dry PC feedstock.

aqueous), noncondensable gas, catalyst coke, catalyst tar, and reactor char. For all combinations of pretreatment, pyrolysis, and catalytic cracking conditions, a two-phase product was generated that included an aqueous phase (~80% $H_2O$) and a heavier, organic phase (i.e., "oily phase"), considered here to be the ultimate product. The liquid product (oily phase) yield (w/w of dry PC shown in panels A and B of Figure 2) decreased significantly with an increasing pretreatment temperature for two temperature comparisons: T225 versus T275 (0.45% difference) and T100 versus T275 (0.27% difference). Although the differences in percentage yield appear small, they are significant relative to the overall yields, which ranged from 0.2 to 3.1% relative to dry biomass. All other pretreatment temperature comparisons were statistically insignificant. Relative to the amount of oil fed, the average liquid product yield (across all catalytic upgrading temperatures) was significantly higher for SP-derived oils (1.9%, w/w of dry PC or 8.5%, w/w of SPO feed) than for FP-derived oils (0.79% of dry PC or 1.7% of FPO feed). The low yield was attributed to the high temperature processing and high catalyst loading used in these experiments intended to maximize BTEX formation. The gas yield significantly increased (at $\alpha$ = 0.05) with an increasing pretreatment temperature for all temperature comparisons ranging from 6 to 32% for FP and from 12.7 to 19.6% for SP.

The average tar yield (Figure 3) also significantly decreased with an increasing catalytic cracking temperature for all pretreatment temperature comparisons, except for T250 (7.3%, w/w of feed) versus T275 (9.0%). Relative to dry biomass for SP (Figure 3A), the tar yield was reduced for all torrefaction temperatures relative to T100 (except for T225 U450), although no differences were seen between individual torrefaction temperatures of T225, T250, and T275. For FP (Figure 3B), the tar yield (%, w/w of dry PC) was reduced with an increasing torrefaction temperature. Within heating rate groups, the torrefaction temperature had a more complex effect on the tar yield relative to oil fed. Within the SP group (Figure 3C) at U450, the tar yield for T225 at 27.8% was significantly higher than for T100 (16.8%), T250 (9.98%), and T725 (17.1%). For SP at U500, the tar yield for T100 at 17.1% was significantly (at $\alpha$ = 0.05) higher than for T225 (9.13%) and T250 (6.75%) but not T275 (11.7%). No significant differences were indicated in the FP group for the various pretreatment temperatures.

A particularly important effect observed was a significant reduction in catalyst coke (Figure 4) with an increasing pretreatment temperature for all temperature comparisons for the whole group (combined slow- and fast-pyrolysis yields). In the best case scenario for SPO upgrading (panels A and C of Figure 3), the reduction in coke (%, w/w of feed) was 28.5% relative to the respective control (SP T250 U450 versus SP T100 U450). For FPO processing, the greatest reduction in coke was 34.9% (FP T275 U400 versus FP T100 U400). All torrefaction temperatures reduced coke and tar compared to T100 controls. The average coke yield (%, w/w of feed) across all upgrading temperatures resulting from FPO processing was

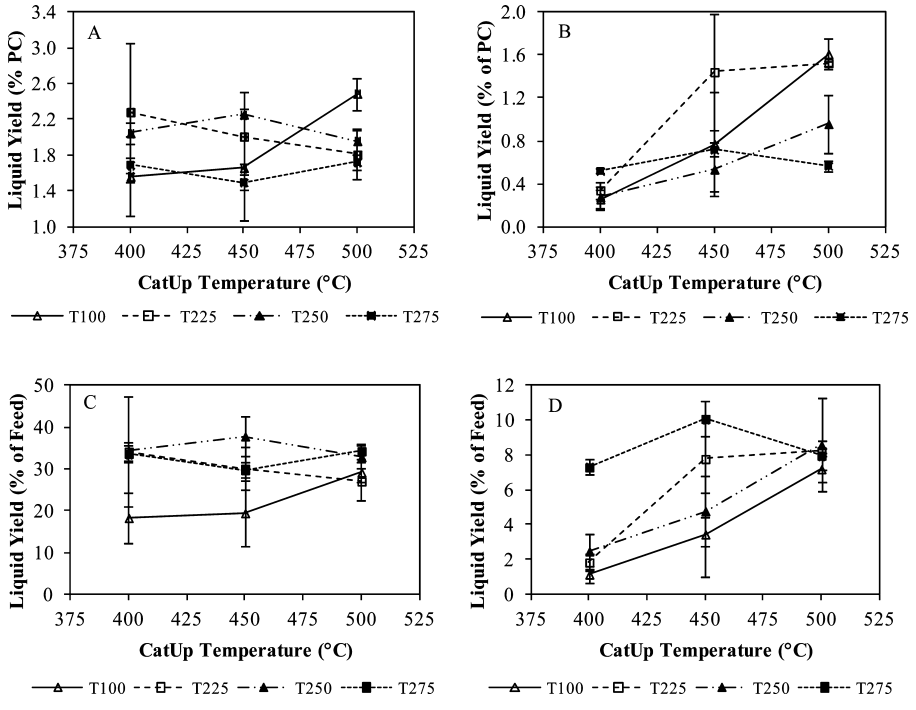


**Figure 2.** Yield (%, w/w) of liquid versus dry PC (A and B) and versus oil fed (C and D) from catalytic cracking of SPO (A and C) and FPO (B and D) derived from PC pretreated at 100, 225, 250, and 275 °C. Error bars indicate the 95% confidence interval.


dx.doi.org/10.1021/ef301694x | *Energy Fuels* 2013, 27, 830–843

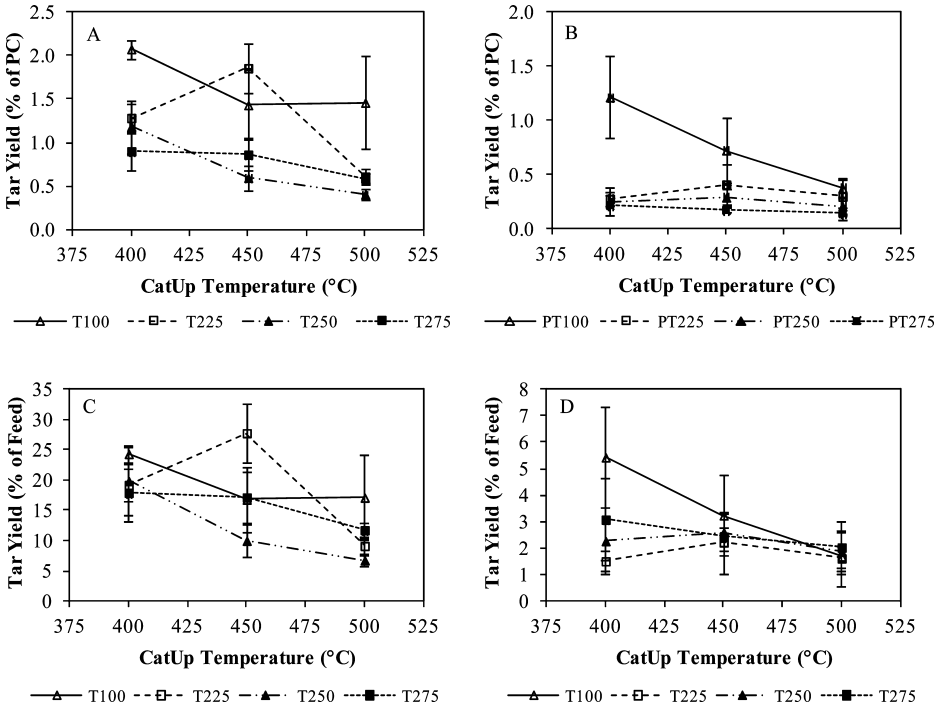


**Figure 3.** Yield (%, w/w) of byproduct tar versus dry PC (A and B) and versus oil fed (C and D) from catalytic cracking of SPO (A and C) and FPO (B and D) derived from PC pretreated at 100, 225, 250, and 275 °C. Error bars indicate the 95% confidence interval.

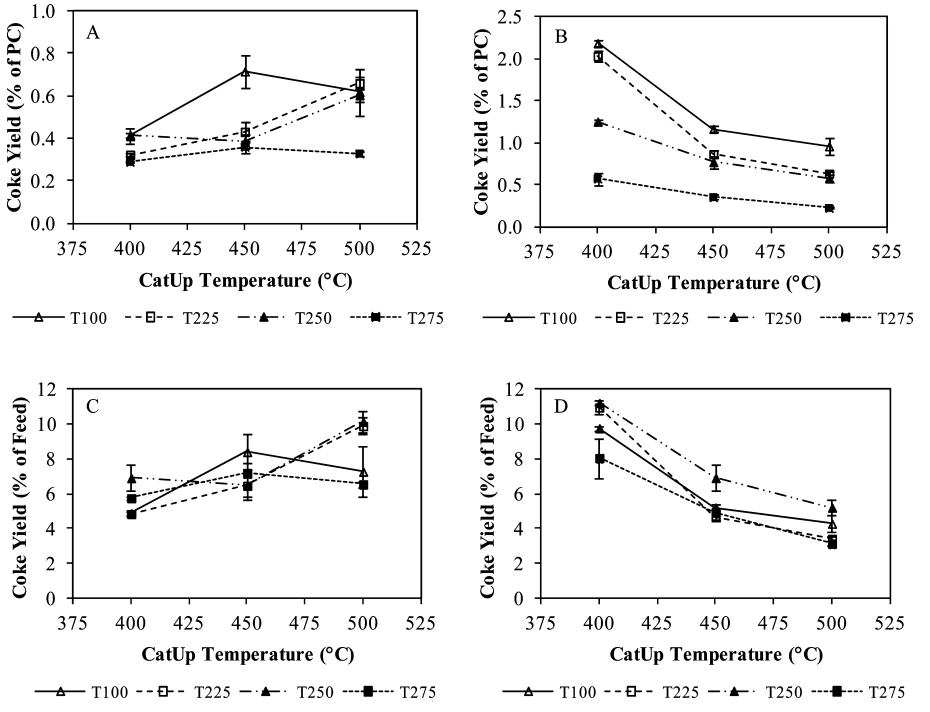


**Figure 4.** Yield (%, w/w) of byproduct coke versus dry PC (A and B) and versus oil fed (C and D) from catalytic cracking of SPO (A and C) and FPO (B and D) derived from PC pretreated at 100, 225, 250, and 275 °C. Error bars indicate the 95% confidence interval.

6.3%, while for SPO processing, the coke yield was 7.2%. The average coke yield (combined average for both FPO- and SPO-derived products) for U400, U450, and U500 was 7.5, 6.3, and 6.4%, respectively. These values are similar to those observed by Vitolo et al.[10] when upgrading Swedish pine-wood-derived bio-oil over HZSM-5 (Si/Al = 50) at 410−490 °C, for which the coke yield (%, w/w of bio-oil) ranged from 4.9 to 6.6%.

When the yield within heating rates is compared, the result was more complex. For U400, significant differences were only observed for FPO-derived byproduct, whereby each of T100 (9.83%, w/w of oil feed), T225 (9.89%), and T250 (10.4%) generated greater amounts of coke than T275 (6.4%). At U450, significant differences were evident for both SP- and FP-derived coke byproduct. For SP, each of T225 (6.71%), T250 (6.18%), and T275 (7.04%) resulted in a reduced coke yield relative to


dx.doi.org/10.1021/ef301694x | Energy Fuels 2013, 27, 830−843

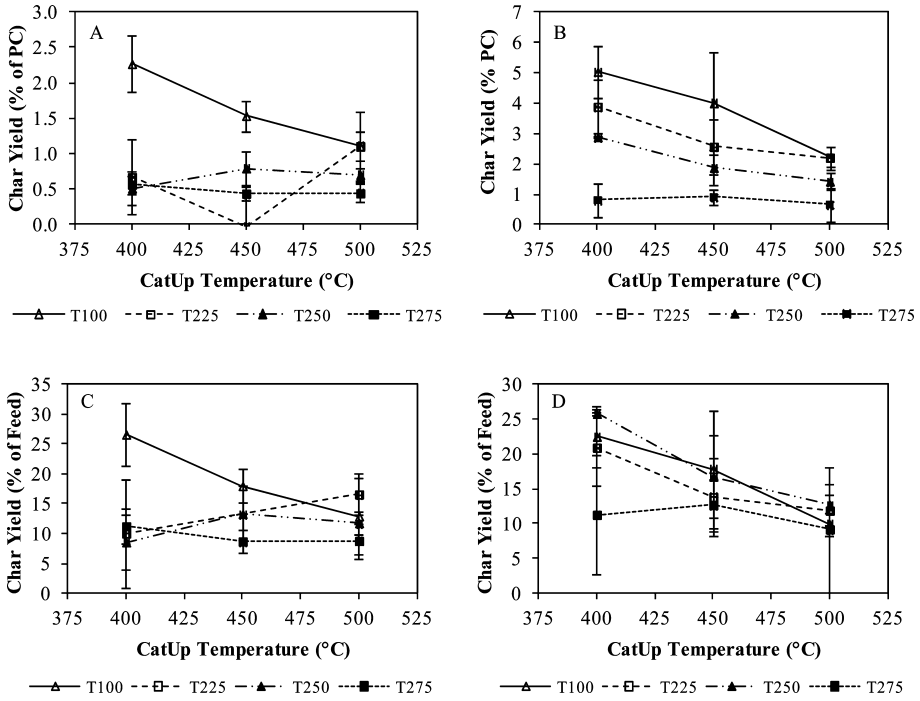


**Figure 5.** Yield (%, w/w) of byproduct char versus dry PC (A and B) and versus oil fed (C and D) from catalytic cracking of SPO (A and C) and FPO (B and D) derived from PC pretreated at 100, 225, 250, and 275 °C. Error bars indicate the 95% confidence interval.

T100 (8.65%), indicating a clear benefit of torrefaction. For FP at U450, T250 pretreatment resulted in a greater coke yield (at 6.54%) than T100 (5.05%), T225 (4.76%), and T275 (5.15%). At U500, only the SP-derived coke yield varied with the pretreatment temperature, with T250 higher (10.5%) than T100 (6.54%) and T275 (6.76%) and T225 higher (9.74%) than T100 (6.54%) and T275 (6.76%). The reasons for the variation in the coke yield as a function of processing conditions, in particular the torrefaction pretreatment temperature, are further explored in the study by Hilten et al.[31]

An increasing torrefaction temperature also significantly reduced reactor average char production relative to dry PC (panels A and B of Figure 5) for all temperature comparisons, except for T225 versus T250. Relative to oil fed (panels C and D of Figure 5), the average char yield was higher for T100 versus T275 and for T250 versus T275, indicating T275 to be an effective processing condition for minimizing reactor char formation. For SP, the largest reduction in char formation relative to oil fed was 61.2% for SP T250 U400 versus SP T100 U400. For FP, the largest reduction was 57.8% for FP T275 U400 versus FP T100 U400.

From a perspective of yield from catalytic cracking, torrefaction was beneficial in the reduction of unwanted byproducts, including tar, char, and coke. For tar in the best performing slow-pyrolysis case, the tar yield (%, w/w of feed) was reduced by 60.5% relative to the respective control (i.e., SP T250 U500 versus SP T100 U500). For FP, tar was reduced by as much as 58% in the best case, FP T225 U400 versus FP T100 U400. For char, a 100% reduction was observed for the best SP case, SP T225 U450 versus SP T100 U450, in comparison to 44% for FP T275 U400 versus FP T100 U400. Coke was reduced by 28.5% for the best SP case, SP T250 U450, in comparison to 35% for FP T275 U400. Product liquid yield was unaffected by torrefaction in any recognizable pattern (i.e., no linear trends were evident), although the gas yield linearly increased with torrefaction because of greater conversion of byproducts. If byproduct minimization (coke, char, and tar) is desired, results showed that pretreatment at 275 °C was the best temperature to use, while pretreatment temperatures at 100, 225, and 250 °C maximized product liquid formation.

**Effect of the Pyrolysis Heating Rate on Product Yield.** The pyrolysis heating rate significantly affected the pyrolysis yield of aqueous phase liquid ($p < 0.001$) and the oily phase liquid ($p < 0.001$), as well as char and noncondensable gas. Aqueous phase liquid formation was eliminated in fast pyrolysis (0%, w/w), whereas for slow-pyrolysis oils, the yield was 27% (w/w of dry PC). As expected, the product liquid yield was significantly increased ($p < 0.001$) as a result of fast-pyrolysis processing (whole oil yield at an average of 14.8%, w/w) relative to slow pyrolysis (organic phase yield at an average of 6.5%, w/w).

Additional yield effects resulting from the pyrolysis heating rate were evident in the secondary catalytic cracking process, as well. Product liquid, noncondensable gas, tar, coke, and char yields were all significantly affected (<0.001 for all) as a function of the pyrolysis heating rate. Product liquid and tar yields were significantly higher and gas, coke, and char yields were lower for SPO versus FPO processing. Figures 2, 3, 4, and 5 show the yield of liquid product, tar, coke, and char, respectively, for both heating rates and all pretreatment temperatures. If maximization of the product and minimization of the byproduct (except tar) is desired, irrespective of product quality, slow pyrolysis is optimal. However, in the FPO processing case, the liquid yield continued to increase at 500 °C and the yield of coke continued to decrease (Figure 4). As such, the processing temperature for liquid product maximization and coke minimization for FPO may be beyond the range attempted here.

**Effect of the Catalytic Upgrading Temperature on Product Yield.** The effect of catalytic cracking on yields of liquid product, tar, coke, and char is also indicated in Figures


dx.doi.org/10.1021/ef301694x | *Energy Fuels* 2013, 27, 830−843

2−5. On average, when taking into consideration all pretreatment temperatures, the liquid product yield significantly increased with an increasing catalytic cracking temperature, although for one individual set of reaction conditions, FP T275 U500 (Figure 2B), the yield was reduced in comparison to lower temperature upgrading. At the same time, the gas yield also significantly increased. Concurrently, tar, coke, and char yields were significantly reduced. Panels A and C and panels B and D of Figure 4 show the yield of coke upon processing SPO and FPO, respectively. At most, the coke yield was around 2.2% (w/w of dry PC) for FPO processed at T100 and U400, and in the best case scenario, the coke yield was ∼0.2% (w/w of dry PC) for FPO processed at T275 and U500. The increase in the liquid yield and the reduction in coke with catalytic cracking temperature were particularly evident during FPO processing. From a process optimization standpoint, if liquid yield maximization and coke minimization were desired, results show that the highest catalytic cracking temperature (500 °C) would be optimal.

**Effect of Process Conditions on Product Quality.** Tables 4 and 5 show characterization results for SP- and FP-derived liquid products, respectively. Intermediate and final product quality was assessed via a variety of measures. First, the changes in elemental C, H, N, S, and O (by difference) and, in particular, $H/C_{eff}$ and O/C ratios as a function of process conditions were used to indicate oil quality. Given CHNS-O values, heating values for oils were also calculated following the study by Channiwala and Parikh.[33] Second, quality was indicated in relation to OOT, an indicator of storage stability. Finally, quality was determined relative to the yield of desirable end-product compounds, specifically BTEX, in the product liquid, as determined via a calibrated GC−MS routine.

**Effect of Process Conditions on CHNS-O, $H/C_{eff}$, O/C, and Higher Heating Value (HHV).** Pretreatment temperature, pyrolysis heating rate, and catalytic cracking temperature all significantly affected elemental C, N, and O as well as the O/C ratio and HHV. Elemental H was affected significantly only by the catalytic upgrading temperature. $H/C_{eff}$ as calculated using eq 1 was significantly affected by both the pyrolysis heating rate and catalytic upgrading temperature. Bio-oil intermediate and end-product characteristics are given in Tables 4 and 5.

The carbon content (i.e., C content) was higher for un-upgraded SPO feedstock than for FPO feedstock. However, for upgraded oils, the carbon content for FPO-derived product was significantly higher (69.9% average versus 69% for SPO-derived product). The C content significantly increased with an increasing catalytic cracking temperature. The FPO T275 U500 product indicated the highest C content at 80.1%. The C content for T275, T250, and T100 were all higher than for T225. In both SPO- and FPO-derived oils, the control had a significantly lower $H/C_{eff}$ ratio than upgraded oils. The SP-derived catalytic upgrading feed oils indicated a higher $H/C_{eff}$ than the FP-derived feed oils. However, for upgraded oils, the results were mixed and there were no statistically significantly differences between $H/C_{eff}$ for SP- and FP-derived product oils. In the best case scenario, $H/C_{eff}$ reached 1.0 in both the FPO T100 U500 and FPO T275 U500 products. The lowest $H/C_{eff}$, at −0.3, was indicated by both the FPO T100 and the FPO T225 feed oils (no catalytic processing). Oils with the highest $H/C_{eff}$ values, at 1.0, corresponded to oils indicating the highest BTEX concentrations ($H/C_{eff}$ for benzene equals 1) observed. The effect was particularly evident in FPO-derived product

**Table 4. Characteristics of Product Bio-oil Generated via Pretreatment, Slow Pyrolysis, and Catalytic Cracking Using Pretreated PC as the Slow-Pyrolysis Feedstock**

| | slow-pyrolysis bio-oil characteristics | | | | | | | | | | | | | | | | | |
|---|---|---|---|---|---|---|---|---|---|---|---|---|---|---|---|---|---|---|
| | T100 | | | | T225 | | | | T250 | | | | T275 | | | | | |
| parameter | T100 feed | U400 | U450 | U500 | T225 feed | U400 | U450 | U500 | T250 feed | U400 | U450 | U500 | T275 feed | U400 | U450 | U500 | | |
| C | 63.4 | 67.9 | 70.1 | 69.0 | 60.5 | 66.4 | 70.8 | 72.4 | 60.8 | 66.8 | 67.0 | 72.3 | 62.4 | 68.4 | 68.0 | 70.0 | | |
| H | 6.3 | 7.8 | 7.9 | 7.6 | 6.5 | 7.1 | 7.9 | 7.7 | 6.5 | 7.6 | 7.4 | 7.7 | 6.2 | 7.4 | 7.7 | 7.9 | | |
| N | 0.2 | 0.1 | 0.0 | 0.0 | 0.7 | 0.3 | 0.4 | 0.5 | 0.5 | 0.2 | 0.0 | 0.2 | 0.2 | 0.2 | 0.1 | 0.0 | | |
| S | 0.0 | 0.0 | 0.0 | 0.0 | 0.0 | 0.0 | 0.0 | 0.0 | 0.0 | 0.0 | 0.0 | 0.0 | 0.0 | 0.0 | 0.0 | 0.0 | | |
| O[a] | 30.1 | 24.3 | 23.4 | 22.2 | 32.4 | 26.3 | 20.9 | 19.8 | 32.2 | 25.5 | 25.6 | 19.7 | 31.2 | 24.1 | 24.2 | 22.1 | | |
| $H/C_{eff}$ | 0.5 | 0.8 | 0.8 | 0.8 | 0.5 | 0.7 | 0.9 | 0.9 | 0.5 | 0.8 | 0.8 | 0.9 | 0.4 | 0.8 | 0.8 | 0.9 | | |
| O/C | 0.4 | 0.3 | 0.3 | 0.2 | 0.4 | 0.3 | 0.2 | 0.2 | 0.4 | 0.3 | 0.3 | 0.2 | 0.4 | 0.3 | 0.3 | 0.2 | | |
| HHV (MJ $kg^{-1}$)[b] | 26.4 | 30.3 | 31.3 | 30.8 | 25.4 | 28.8 | 31.9 | 32.4 | 25.5 | 29.6 | 29.5 | 32.3 | 25.8 | 30.0 | 30.2 | 31.4 | | |
| $H_2O$ (%) | 6.7 | N/A | 4.1 | N/A | 9.1 | N/A | 4.1 | N/A | 2.6 | N/A | 4.1 | N/A | 8.0 | N/A | 5.5 | N/A | | |
| OOT (°C) | 161.5 | 145.5 | 160.5 | 163.9 | 157.1 | 145.5 | 160.5 | 156.5 | 159.4 | 140.9 | 151.4 | 156.6 | 158.0 | 153.0 | 154.5 | 160.4 | | |

[a]Calculated by difference. [b]Calculated following the study by Channiwala and Parikh.[33]



dx.doi.org/10.1021/ef301694x | Energy Fuels 2013, 27, 830−843

Table 5. Characteristics of Product Bio-oil Generated via Pretreatment, Fast Pyrolysis, and Catalytic Cracking Using Pretreated PC as the Fast-Pyrolysis Feedstock

| | fast-pyrolysis bio-oil characteristics | | | | | | | | | | | | | | |
|---|---|---|---|---|---|---|---|---|---|---|---|---|---|---|---|
| | T100 | | | | T225 | | | | T250 | | | | T275 | | | |
| parameter | T100 feed | U400 | U450 | U500 | T225 feed | U400 | U450 | U500 | T250 feed | U400 | U450 | U500 | T275 feed | U400 | U450 | U500 |
| C | 35.1 | 71.6 | 74.2 | 80.4 | 35.8 | 39.7 | 57.2 | 71.9 | 39.3 | 71.5 | 72.7 | 71.1 | 42.0 | 75.6 | 72.0 | 80.1 |
| H | 6.5 | 7.9 | 7.8 | 8.1 | 6.2 | 8.8 | 7.9 | 7.0 | 6.1 | 7.5 | 7.7 | 7.7 | 6.0 | 7.4 | 7.6 | 8.0 |
| N | 0.0 | 0.0 | 0.0 | 0.0 | 0.1 | 0.0 | 0.0 | 0.1 | 0.2 | 0.0 | 0.0 | 0.0 | 0.1 | 0.0 | 0.0 | 0.0 |
| S | 0.0 | 0.0 | 0.0 | 0.0 | 0.0 | 0.0 | 0.0 | 0.0 | 0.0 | 0.0 | 0.0 | 0.0 | 0.0 | 0.0 | 0.0 | 0.0 |
| O[a] | 58.4 | 33.1 | 18.0 | 11.6 | 57.9 | 53.6 | 34.9 | 21.1 | 53.8 | 32.0 | 19.6 | 20.7 | 52.0 | 18.8 | 20.4 | 11.9 |
| $H/C_{eff}$ | −0.3 | 0.6 | 0.9 | 1.0 | −0.3 | 0.6 | 0.7 | 0.7 | −0.2 | 0.6 | 0.9 | 0.9 | −0.2 | 0.8 | 0.8 | 1.0 |
| O/C | 1.3 | 0.3 | 0.2 | 0.1 | 1.2 | 1.0 | 0.5 | 0.2 | 1.0 | 0.3 | 0.2 | 0.2 | 0.9 | 0.2 | 0.2 | 0.1 |
| HHV (MJ $kg^{-1}$)[b] | 13.9 | 30.9 | 33.2 | 36.4 | 13.8 | 18.7 | 25.7 | 31.1 | 15.4 | 30.5 | 32.5 | 31.7 | 16.3 | 33.2 | 32.0 | 36.2 |
| $H_2O$ (%) | 18.7 | N/A | 1.2 | N/A | 24.6 | N/A | 8.5 | N/A | 19.4 | N/A | 2.6 | N/A | 21.0 | N/A | 7.5 | N/A |
| OOT (°C) | 168.6 | 161.0 | 160.7 | 159.7 | 135.8 | 145.9 | 157.7 | 163.3 | 130.0 | 162.2 | 154.9 | 164.9 | 126.4 | 149.7 | 151.2 | 149.1 |

[a]Calculated by difference. [b]Calculated following the study by Channiwala and Parikh.[33]

(Figure 8D). For FPO T275 U500, the concentration of BTEX was approximately 100 g $L^{-1}$, whereas for the SPO-derived product (Figure 8B), the concentration was at most 50 g $L^{-1}$.

A reduction of O/C is a good indicator of deoxygenation. The catalytic upgrading process significantly reduced O/C in bio-oils from all preprocessing and pyrolysis processing conditions relative to the feed oils. For SPO and FPO feedstocks, the average O/C was 0.75 versus 0.275 for upgraded oils, a reduction of 63%. Overall, SP-derived oils had lower O/C than FP-derived oils at 0.29 versus 0.49. As a function of torrefaction, a significant reduction in O/C was seen for T100, T250, and T275 relative to T225. No other pretreatment temperature comparisons indicated significant differences. As such, it was concluded that torrefaction pretreatment had no clear effect on O/C. However, the temperature at which catalytic cracking was performed significantly impacted O/C. Bio-oils from all upgrading temperatures had lower O/C than the non-catalytically cracked bio-oil control (O/C = 0.75). In addition, U500 bio-oil showed reduced O/C relative to U400, averaging 0.18 versus 0.375 for U400, a reduction of 53%. Results indicated that torrefaction pretreatment did not significantly affect O/C, although catalytic upgrading was effective at all upgrading temperatures relative to the control.

HHV (Tables 4 and 5), a good indicator of the potential applicability of pyrolysis oils in combustion applications, was impacted by process conditions in a multitude of ways. HHV increased with an increasing catalytic processing temperature for all temperature comparisons, except for U500 versus U450. Within heating rate groups, HHV varied significantly. For SP, higher catalytic cracking temperature resulted in a significantly higher HHV, except for U450 (30.7 MJ $kg^{-1}$) versus CTRL (25.8 MJ $kg^{-1}$), U400 (29.7 MJ $kg^{-1}$) versus CTRL (25.8 MJ $kg^{-1}$), and U500 (31.7 MJ $kg^{-1}$) versus U450 (25.8 MJ $kg^{-1}$). The greatest difference in HHV for SP oils was between U500 and the control (6.0 MJ $kg^{-1}$ difference). For FP-derived oils, the same was true. U500 showed the highest HHV relative to the control (18.9 MJ $kg^{-1}$ increase). Within catalytic processing temperature groups, HHV varied as a result of the pyrolysis heating rate. Within the catalytic cracking control group, HHV for SPO (25.8 MJ $kg^{-1}$) was significantly higher than for FPO (14.9 MJ $kg^{-1}$). However, for all other catalytic processing temperatures, including U400, U450, and U500, the HHV for upgraded FPO was significantly higher at 28.3, 30.9, and 33.9 MJ $kg^{-1}$, respectively.

**Effect of Process Conditions on OOT.** All process variables (i.e., pyrolysis heating rate, pretreatment temperature, and catalytic cracking temperature) significantly affected the storage stability of the product liquids as measured via OOT (values shown in Tables 4 and 5). OOT for SP-derived oils was significantly ($p$ = 0.024) higher (at an average of 155.3 °C) than for FP-derived oils (152.6 °C). This was assumed to be due to the fact that fast-pyrolysis oils, by nature, exist at an unsteady state and will change over time, thus lacking storage stability.[33] Because slow pyrolysis drives reactions further to completion because of longer contact times, the SP oils would conceivably be more stable. Catalytic cracking temperature comparisons indicated that OOT for U500 (159.3 °C) was higher than the control (149.6 °C) and U400 (150.5 °C) and OOT for U450 was higher than the control (149.6 °C) and U400 (150.5 °C). OOT for T100 bio-oils (160.2 °C) was significantly greater than for oils derived from T225 (152.8 °C), T250 (152.5 °C), or T275 (150.3 °C). These results indicated

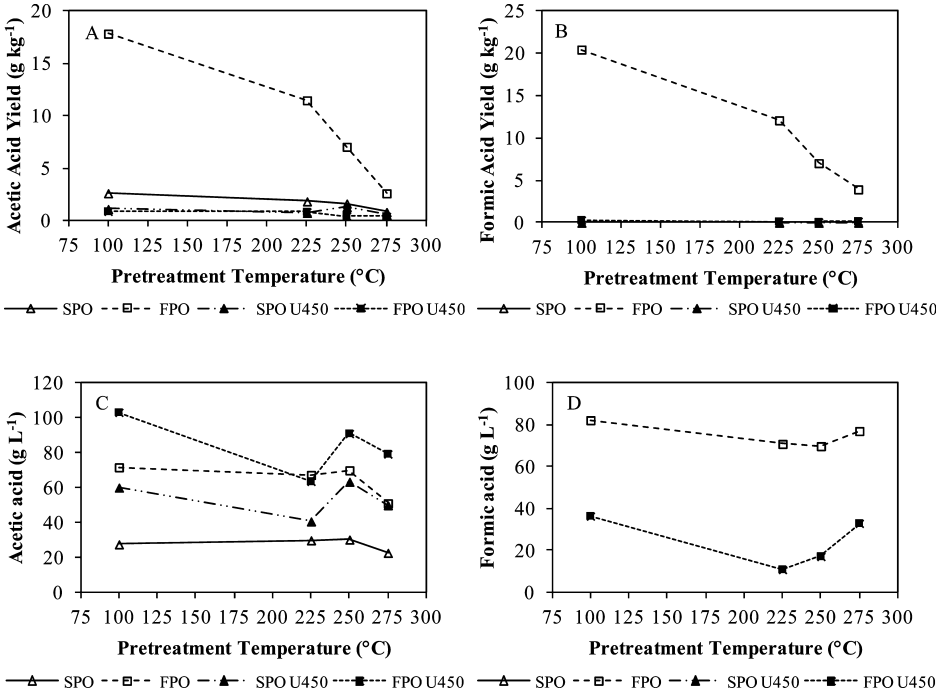


**Figure 6.** Yield (A and B, in g $kg^{-1}$ of dry PC) and concentration (C and D, in g $L^{-1}$) of acetic acid (A and C) and formic acid (B and D) in bio-oil generated from feedstock pretreated at 100, 225, 250, and 275 °C prior to and after catalytic cracking, as determined by HPLC.

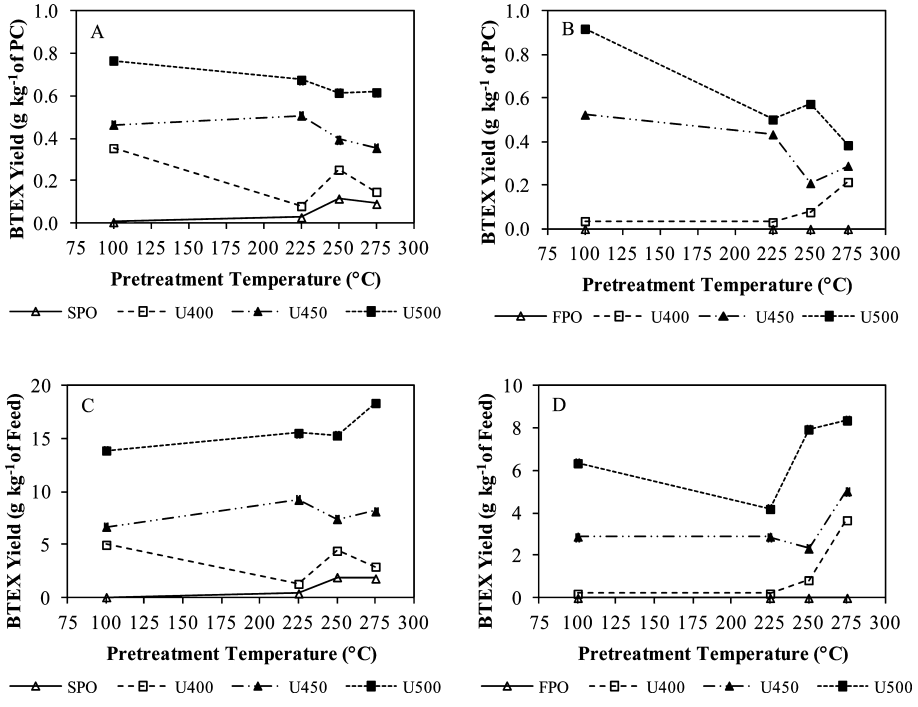


**Figure 7.** Yield (%, w/w) of BTEX versus dry PC (A and B) and versus oil fed (C and D) from catalytic cracking of SPO (A and C) and FPO (B and D) derived from PC pretreated at 100, 225, 250, and 275 °C. Error bars indicate the 95% confidence interval.

that torrefaction pretreatment had a negative effect on product stability relative to the non-torrefied control; i.e., OOT decreased with an increasing torrefaction temperature. In the best case scenario, the OOT for bio-oil derived from torrefied feedstock was 7.3 °C lower than the control (for U225), and in the worst case, the difference was 10.5 °C (for T275). However, there was no significant difference in OOT among oils derived from torrefied feedstock. On the other hand, catalytic cracking did have a positive effect on OOT at all catalytic processing temperatures. In the best case scenario, OOT was 10.3 °C higher (for U500) relative to the control, although no differences were significant among oils processed at different catalytic upgrading temperatures.

**Effect of Process Conditions on Acetic and Formic Acids.** Acetic and formic acids are the highest concentration organic acids in bio-oil. These acids cause high acidity and corrosivity, thereby limiting the range of applications for bio-oil. It was proposed that torrefaction pretreatment would drive


dx.doi.org/10.1021/ef301694x | *Energy Fuels* 2013, 27, 830−843

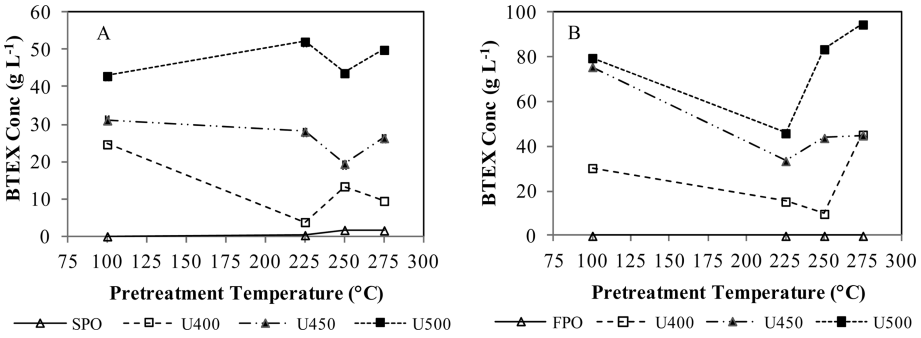


**Figure 8.** BTEX concentration (g $L^{-1}$) in (A) SPO and (B) FPO generated from pretreated feedstock prior to and after catalytic cracking at 400, 450, or 500 °C, as determined by GC–MS.

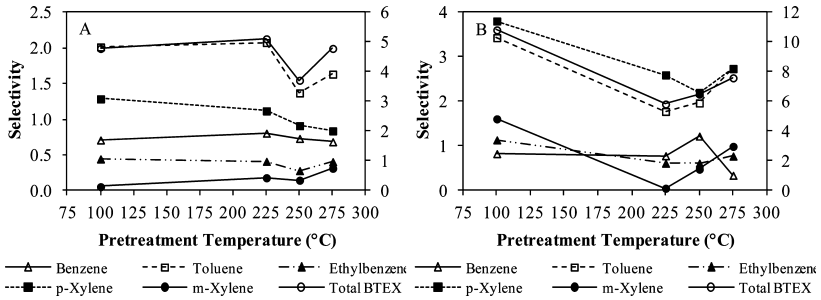


**Figure 9.** Selectivity (%, db) for BTEX components and combined BTEX in (A) SPO- and (B) FPO-derived product liquid from catalytic processing at 450 °C. Total BTEX is plotted on the right-hand axis.

away organic acids prior to pyrolysis and upgrading treatments, leading to reduced concentrations and yields in bio-oil intermediates and the end-product (and potentially higher pH).

From panels A and B of Figure 6, it is clear that the yield of acetic and formic acids (in g $kg^{-1}$ of dry PC) decreases with an increasing torrefaction temperature. For FPO, the yields of acetic and formic acids in non-upgraded bio-oil decrease from 18 to 2.6 g $kg^{-1}$ and from 20.5 to 3.9 g $kg^{-1}$, respectively. Consequently, the yields of acetic and formic acids in the upgraded product (U450) were reduced as well, to less than 1 g $kg^{-1}$ for each. For SPO, the yield of acetic acid in non-torrefied, non-upgraded feedstock was lower at 2.6 g $kg^{-1}$. Formic acid was not detected in either the SPO feed oils or the upgraded oils at any torrefaction temperature. The acetic acid yield lowered to 0.82 g $kg^{-1}$ for bio-oil generated from SPO T275 and to 0.54 g $kg^{-1}$ for SPO T275 U450.

As seen in panels C and D of Figure 6, the concentrations of acetic and formic acids varied quite a bit for FP feed oils and FP U450 products. As a function of catalytic cracking, the formic acid concentration was reduced for both FPO and SPO after processing at U450 but increased for acetic acid. For FPO feedstock, the average concentrations of acetic and formic acids were 65.0 and 75.0 g $L^{-1}$, respectively. After catalytic processing at U450, concentrations were 84.3 and 24.4 g $L^{-1}$, respectively. Although the acetic acid concentration did not decrease and, in fact, increased somewhat, the large decrease in the formic acid concentration reduced the combined acid concentration in upgraded FPO.

Torrefaction significantly reduced both acetic and formic acid concentrations from 71.7 to 51.1 g $L^{-1}$ (T100 versus T275) and from 82.2 to 69.8 g $L^{-1}$ (T100 versus T250), respectively, in FP feed oils. For SP feed oil, the concentration of acetic acid was least in the T275 oil, at 22.7 g $L^{-1}$, and highest in T250, at 30.4 g $L^{-1}$. Formic acid was not detected. In upgraded SPO, the acetic acid concentration increased to 53.5 g $L^{-1}$, indicating that catalytic processing at conditions used here did not convert acids effectively.

**Effect of Process Conditions on BTEX.** The yield of BTEX (g $kg^{-1}$ of dry PC) is shown in panels A (SPO feedstock) and B (FPO feedstock) of Figure 7. The yield of BTEX (%, w/w of oil feed) is shown in panels C (SPO) and D (FPO) of Figure 7. The yield (g $kg^{-1}$ of dry PC) increased with an increasing catalytic processing temperature, with increases from 0.21 to 0.67 g $kg^{-1}$ for SPO and from 0.09 to 0.59 g $kg^{-1}$ for FPO for U400 versus U500. Neither torrefaction or heating rate had a significant effect on the BTEX yield.

The concentration of BTEX in feed and product liquid is provided in panels A (SPO feedstock) and B (FPO feedstock) of Figure 8. The average BTEX concentration was significantly higher in FPO- versus SPO-derived product at 50.1 and 28.8 g $L^{-1}$, respectively. The BTEX concentration in non-upgraded SPO and FPO was minimal at 0.96 and 0.0 g $L^{-1}$, respectively. The concentration increased with an increasing catalytic cracking temperature from 25.2 to 75.8 g $L^{-1}$ for FPO and from 12.9 to 47.2 g $L^{-1}$ for SPO. The torrefaction temperature did not significantly affect the BTEX concentration. The concentration of guaiacol and creosol (data not shown; see the study by Hilten et al.[31]) in the feed oils did not have a significant effect on the BTEX concentration, meaning that the concentration of other components and process conditions, in particular the catalytic processing temperature, were the major determinants.

**Effect of Process Conditions on BTEX Selectivity.** Figure 9 shows catalyst selectivity for BTEX compounds, including benzene, toluene, ethylbenzene, *p*-xylene, *m*-xylene, and total BTEX, on a dry basis [i.e., dry yield of components/(dry feed − dry yield of components)].


dx.doi.org/10.1021/ef301694x | *Energy Fuels* 2013, 27, 830–843

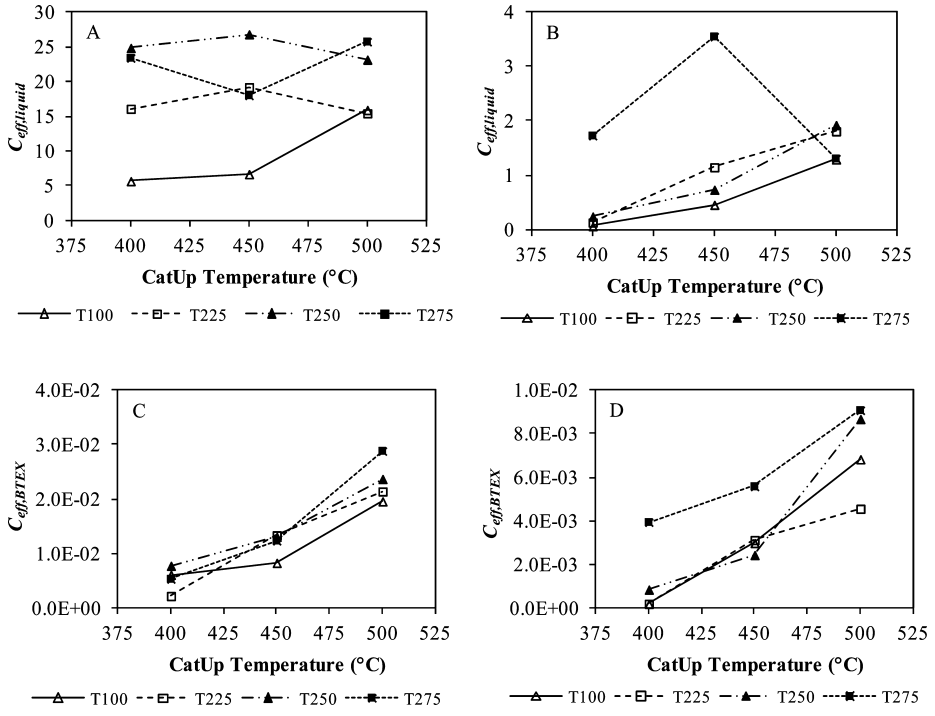


**Figure 10.** Catalyst effectiveness, $C_{eff}$ (%, wb), for liquid (A and B) and BTEX (C and D) production via HZSM-5 processing of SPO (A and C) and FPO (C and D) derived from PC pretreated at 100, 225, 250, and 275 °C.

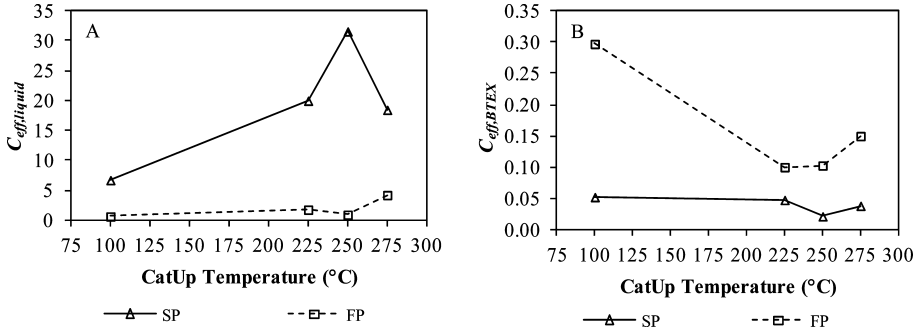


**Figure 11.** Catalyst effectiveness, $C_{eff}$ (%, db), for total liquid (A) and BTEX (B) production via HZSM-5 processing of SPO and FPO derived from PC pretreated at 100, 225, 250, and 275 °C and U450.

**Effect of Process Conditions on Catalyst Effectiveness.** Three-way ANOVA tests were also used to determine if independent variables, including torrefaction temperature, pyrolysis heating rate, and catalytic cracking temperature, significantly affected catalyst effectiveness (on a wet basis) for the production of liquid product (panels A and B of Figure 10) and BTEX product (panels C and D of Figure 10), in particular. Catalyst effectiveness for liquid production, $C_{eff,liquid}$, was significantly affected by the heating rate and pretreatment temperature but not by the catalytic cracking temperature. However, there was significant interaction between the heating rate and pretreatment temperature. As such, a two-way ANOVA was used on the two groups, SPO and FPO processed, separately. For SPO (Figure 10A), the pretreatment temperature had a significant positive effect on liquid production effectiveness; i.e., $C_{eff,liquid}$ increased with an increasing processing temperature. The catalytic cracking temperature did not have a significant effect on $C_{eff,liquid}$ for SPO. For FPO (Figure 10B), pretreatment and the catalytic cracking temperature significantly affected $C_{eff,liquid}$. The mean effectiveness was 0.485, 0.885, 0.701, and 1.202 for T100, T225, T250, and T275, respectively, indicating an increase in effectiveness of 148% in the best case scenario relative to the control, T100. The mean effectiveness was 0.201, 0.921, and 1.332 for U400, U450, and U500, respectively, indicating a 503% increase for U500 versus U400. Thus, both pretreatment temperature and catalytic cracking temperature had a positive linear effect on $C_{eff,liquid}$. If maximizing the liquid yield relative to SPO or FPO feed is desired, pretreatment at 275 °C and catalytic processing at 500 °C are optimal.

Panels A and B of Figure 11 show that catalyst effectiveness for BTEX production, $C_{eff,BTEX}$, increases with increasing catalytic cracking for both SPO and FPO. Three-way ANOVA analysis indicated that both the heating rate and catalytic cracking temperature had a significant effect on $C_{eff,BTEX}$. The difference in average $C_{eff,BTEX}$ for SPO versus FPO was 9.6, meaning that the catalyst was significantly more effective at processing SPO. This is likely due to the high water content in FPO that cannot be converted to BTEX and, in practice, dilutes species that would form BTEX. However, the final concentration of BTEX in FPO-derived product was higher (Figure 8). A better comparison was possible between


dx.doi.org/10.1021/ef301694x | Energy Fuels 2013, 27, 830−843

processing conditions within each group of the pyrolysis heating rate. Within both SPO- and FPO-processing groups, torrefaction had no significant impact on $C_{eff,BTEX}$. The catalytic cracking temperature had a major effect, however, indicating a linear increase with the increasing processing temperature. For the case of the best performing process condition for SPO (T275 U500), an increase in $C_{eff,BTEX}$ ($\times 10^{-2}$) from 2.5 (T100 U400) to 36.6 (T275 U500) was seen. For FPO, the increase from 0.004 to 7.0 was observed. The conclusion was that HZSM-5 was significantly more effective at generating BTEX at the upper end of the catalytic cracking processing temperature range attempted here for both SPO and FPO processing.

## ■ CONCLUSION

Biomass torrefaction was proposed to improve the yield, quality, stability, and catalytic treatability of slow- and fast-pyrolysis oils. The actual effects were mixed with some positive, some negative, and some neutral results. As expected, torrefaction reduced the total liquid yield of bio-oil and increased the solid yield upon pyrolysis because of the removal of volatile components. The torrefied feedstock exhibited an increased carbon content and heating value. We proposed that torrefaction would reduce coking upon cracking, but we observed a dramatic reduction in not only coke but also reactor char and tar as well, with very positive effects. Torrefaction at 275 °C minimized reactor char, catalyst coke, and tar most effectively. Catalyst effectiveness for both liquid and BTEX production was improved with an increasing torrefaction temperature relative to the control. Both effectiveness and BTEX concentration were highest in liquid product derived from feedstock torrefied at 275 °C. One negative effect of torrefaction was a reduction in oxidative stability, as measured by the oxidation onset temperature. However, a more in-depth study of stability is needed to truly claim that torrefaction reduces stability. For most measures of quality, including O/C ratio, $H/C_{eff}$, and HHV, torrefaction had no significant effect.

In summary, torrefaction pretreatment appeared to be most effective at improving treatability of liquid feedstock. Although grinding energy for size reduction was not measured here, reduction in grinding energy has been well-documented for torrefied biomass. Pretreatment clearly improved catalytic upgrading by reducing the yield of byproducts, most notably for catalyst coke, the formation of which has severely limited the commercial potential of processing bio-oil via catalytic cracking.

## ■ AUTHOR INFORMATION

### Corresponding Author

*Telephone: +1-706-542-0940. Fax: +1-706-542-8806. E-mail: rog@uga.edu.

### Notes

The authors declare no competing financial interest.

## ■ REFERENCES

(1) Chen, G.; Andries, J.; Luo, Z.; Spliethoff, H. Biomass pyrolysis/gasification for product gas production: The overall investigation of parametric effects. *Energy Convers. Manage.* **2003**, *44*, 1875−1884.

(2) Carlson, T.; Cheng, Y.; Jae, J.; Huber, G. Production of green aromatics and olefins by catalytic fast pyrolysis of wood sawdust. *Energy Environ. Sci.* **2011**, *4*, 145−161.

(3) Valle, B.; Gayubo, A.; Atutxa, A.; Alonso, A.; Bilbao, J. Integration of thermal and catalytic transformation for upgrading biomass pyrolysis oil. *Int. J. Chem. React. Eng.* **2007**, *5*, 1−10.

(4) Adjaye, J.; Bakhshi, N. Production of hydrocarbons by catalytic upgrading of a fast pyrolysis bio-oil. Part II: Comparative catalyst performance and reaction pathways. *Fuel Process. Technol.* **1995**, *45*, 185−202.

(5) Adjaye, J.; Bakhshi, N. Production of hydrocarbons by catalytic upgrading of a fast pyrolysis bio-oil. Part I: Conversion over various catalysts. *Fuel Process. Technol.* **1995**, *45*, 161−183.

(6) Lu, Q.; Zhang, Y.; Tang, Z.; Li, W.; Zhu, X. Catalytic upgrading of biomass fast pyrolysis vapors with titania and zirconia/titania based catalysts. *Fuel* **2010**, *89*, 2096−2103.

(7) Corma, A.; Huber, G.; Sauvanaud, L.; O'Connor, P. Processing biomass-derived oxygenates in the oil refinery: Catalytic cracking (FCC) reaction pathways and role of catalyst. *J. Catal.* **2007**, *247*, 302−327.

(8) Park, H.; Heo, H.; Jeon, J.; Kim, J.; Ryoo, R.; Jeong, K.; Park, Y. Highly valuable chemicals production from catalytic upgrading of radiate pine saw dust-derived pyrolytic vapors over mesoporous MFI zeolites. *Appl. Catal., B* **2010**, *95*, 365−373.

(9) Elliott, D. C.; Neuenschwander, G. G. Liquid fuels by low-severity hydrotreating of biocrude. In *Developments in Thermochemical Biomass Conversion*; Bridgwater, A. V., Boocock, D. G. B., Eds.; Blackie Academic and Professional: London, U.K., 1996; Vol. *1*, pp 611−621.

(10) Vitolo, S.; Bresci, B.; Seggiani, M.; Gallo, M. Catalytic upgrading of pyrolytic oils over HZSM-5 zeolite: Behaviour of the catalyst when used in repeated upgrading−regenerating cycles. *Fuel* **2001**, *80*, 17−26.

(11) Rao, M.; Soni, D.; Sieli, G. Convert bottom-of-the-barrel into diesel and light olefins. *Hydrocarbon Process.* **2011**, *February*, 45−49.

(12) Gayubo, A.; Aguayo, A.; Atutxa, A.; Valle, B.; Bilbao, J. Undesired components in the transformation of biomass pyrolysis oil into hydrocarbons on an HZSM-5 zeolite catalyst. *J. Chem. Technol. Biotechnol.* **2005**, *80*, 1244−1251.

(13) Gagnon, J.; Kaliaguine, S. Catalytic hydrotreatment of vacuum pyrolysis oils from wood. *Ind. Eng. Chem. Res.* **1988**, *27* (10), 1783−1788.

(14) Laurent, E.; Delmon, B. Study of the hydrodeoxygenation of carbonyl, carboxylic and guaiacyl groups over sulfided $CoMo/\gamma\text{-}Al_2O_3$ and $NiMo/\gamma\text{-}Al_2O_3$ catalysts: I. Catalytic reaction schemes. *Appl. Catal., A* **1994**, *109* (1), 77−96.

(15) Centeno, A.; Laurent, E.; Delmon, B. Influence of the support of CoMo sulfide catalysts and of the addition of potassium and platinum on the catalytic performances for the hydrodeoxygenation of carbonyl, carboxyl, and guaiacol-type molecules. *J. Catal.* **1995**, *154*, 288−298.

(16) Wildschut, J.; Mahfud, F.; Venderbosch, R.; Heeres, H. Hydrotreatment of fast pyrolysis oil using heterogeneous noble-metal catalysts. *Ind. Eng. Chem. Res.* **2009**, *48*, 10324−10334.

(17) Gayubo, A.; Valle, B.; Aguayo, A.; Olazar, M.; Bilbao, J. Pyrolytic lignin removal for the valorization of biomass pyrolysis crude bio-oil by catalytic transformation. *J. Chem. Technol. Biotechnol.* **2010**, *85*, 132−144.

(18) Phanphanich, M.; Mani, S. Impact of torrefaction on the grindability and fuel characteristics of forest biomass. *Bioresour. Technol.* **2010**, *102*, 1246−1253.

(19) Tumuluru, J.; Sokhansanj, S.; Wright, C.; Kremer, T. GC analysis of volatiles and other products from biomass torrefaction process. In *Advanced Gas Chromatography—Progress in Agricultural, Biomedical and Industrial Applications*; Mohd, M., Ed.; InTech: Rijeka, Croatia, 2012; pp 211−234.

(20) Bergman, P.; Keil, J. Torrefaction for biomass upgrading. *Proceedings of the 14th European Biomass Conference and Exhibition*; Paris, France, Oct 17−21, 2005.

(21) Pommer, L.; Gerber, L.; Olofsson, I.; Wiklund-Lindstrom, S.; Nordin, A. Gas composition from biomass torrefaction—Preliminary results. *Proceedings of the 19th European Biomass Conference and Exhibition*; Berlin, Germany, June 6−10, 2011.

(22) Mani, S.; Das, K. C.; Kastner, J. *Development of Biomass Torrefaction Technology To Produce Biocoal for Electricity Production*, Final Report to State of Georgia; Georgia Traditional Industries Program: Atlanta, GA, 2009.
(23) Meng, J.; Park, J.; Tilotta, D.; Park, S. The effect of torrefaction on the chemistry of fast-pyrolysis bio-oil. *Bioresour. Technol.* **2012**, *111*, 439−446.
(24) Gayubo, A.; Aguayo, A.; Atutxa, A.; Prieto, R.; Bilbao, J. Deactivation of a HZSM-5 zeolite catalyst in the transformation of the aqueous fraction of biomass pyrolysis oil into hydrocarbons. *Energy Fuels* **2004**, *18*, 1640−1647.
(25) National Science Foundation (NSF). *Breaking the Chemical and Engineering Barriers to Lignocellulosic Biofuels: Next Generation Hydrocarbon Biorefineries*; Huber, G. W., Ed.; NSF: Washington, D.C.; 2008; p 180.
(26) de Wild, P.; Uil, H.; Reith, J.; Kiel, J.; Heeres, H. Biomass valorisation by staged degasification: A new pyrolysis-based thermochemical conversion option to produce value-added chemicals from lignocellulosic biomass. *J. Anal. Appl. Pyrolysis* **2009**, *85*, 124−133.
(27) Zheng, A.; Zhao, Z.; Chang, S.; Huang, Z.; He, F.; Li, H. Effect of torrefaction temperature on product distribution from two-staged pyrolysis of biomass. *Energy Fuels* **2012**, *26* (5), 2968−2974.
(28) Prins, M.; Ptasinski, K.; Janssen, F. Torrefaction of wood: Part 2—Analysis of products. *J. Anal. Appl. Pyrolysis* **2006**, *77* (1), 35−40.
(29) Perego, C.; Bosetti, A. Biomass to fuels: The role of zeolite and mesoporous materials. *Microporous Mesoporous Mater.* **2011**, *144*, 28−39.
(30) Joo, O.; Jung, K.; Han, S. Modification of H-ZSM-5 and $\gamma$-alumina with formaldehyde and its application to the synthesis of dimethyl ether from syn-gas. *Bull. Korean Chem. Soc.* **2002**, *23* (8), 1103−1105.
(31) Hilten, R.; Speir, R.; Kastner, J.; Mani, S.; Das, K. C. Effect of torrefaction on bio-oil upgrading over HZSM-5. Part 2: Byproduct formation and catalyst properties and function. *Energy Fuels* **2012**, DOI: 10.1021/ef301695c.
(32) Hilten, R.; Das, K. C. Comparison of three accelerated aging procedures to assess bio-oil stability. *Fuel* **2010**, *89*, 2741−2749.
(33) Channiwala, S.; Parikh, P. A unified correlation for estimating HHV of solid, liquid and gaseous fuels. *Fuel* **2002**, *81*, 1051−1063.